ChemComm

COMMUNICATION

View Article Online
View Journal | View Issue

Cite this: *Chem. Commun.*, 2019, 55, 4059

Received 1st March 2019,
Accepted 7th March 2019

DOI: 10.1039/c9cc01701a

rsc.li/chemcomm

Design of a Zn-MOF biosensor *via* a ligand "lock" for the recognition and distinction of S-containing amino acids†

Xiao-Qin Wu,[ab] Yan Liu,[b] Pei-Qi Feng,[a] Xue-Hong Wei,[a] Guang-Ming Yang,[b] Xiao-Hang Qiu*[b] and Jian-Gong Ma *[b]

Two new 2D Zn(II) metal–organic frameworks (MOFs) $\{[Zn_2(L)_2(\mu_2\text{-}O)(H_2O)_3]\cdot 3DMA\}_n$ (Zn-1) and $[Zn_2(L)_2(2,2'\text{-bipy})(\mu_2\text{-}O)(H_2O)_2]_n$ (Zn-2) (H_2L = 2,5-thiophene dicarboxylic acid, bipy = 2,2′-dipyridyl) were designed and synthesized. Through the strategy of introducing bipy as a "lock", Zn-1 was transferred to Zn-2 *via* a crystal-to-crystal process, which showed significantly enhanced solvent and air stability compared to that of Zn-1. Without post modification, Zn-2 was used as an electrode modified material to construct sensors for the electrochemical recognition and distinction of S-containing amino acids, including L-cysteine, L-methionine and L-cystine.

Metal–organic frameworks (MOFs), known as crystalline materials with multi-dimensional frameworks constructed upon joining metal centers with organic linkers, have developed rapidly due to their fascinating structures, unique properties, and applications in many fields.[1–6] Most recently, MOFs have started to attract increasing attention in the area of electrochemical sensors.[7–12] The electrochemical reaction mechanism between MOFs and guest molecules occurs *via* two approaches: one is target molecules diffuse into the pores/channels of MOFs with corresponding shape- and size-selectivity over the incorporated guests; another approach originates from the chemically specific interactions between the frameworks and guest molecules such as hydrogen bonding, π–π interactions, bare metal sites, and van der Waals interactions.[13]

Despite the excellent properties of MOFs that suggest them as candidates for electrode modified materials, it is a great challenge to design and synthesize MOF sensors, because it is quite difficult to guarantee MOFs' electrochemical activities and good stabilities at the same time, and MOFs directly used as electrochemical sensors without further modification have been reported quite rarely at present.[7,14–17] As a result, improvement of the stability of the electro-active MOFs is one of the essential challenges for MOF sensors. Herein, we report a new method to design and synthesise a MOF sensor *via* introducing a 'lock' ligand into the frame of MOFs. Two 2D Zn-MOFs, namely $\{[Zn_2(L)_2(\mu_2\text{-}O)(H_2O)_3]\cdot 3DMA\}_n$ (**Zn-1**) and $[Zn_2(L)_2(2,2'\text{-bipy})(\mu_2\text{-}O)(H_2O)_2]_n$ (**Zn-2**) (H_2L = 2,5-thiophene dicarboxylic acid, bipy = 2,2′-dipyridyl) were obtained. Through the introduction of bipy as a "lock", **Zn-1** was successfully transferred to **Zn-2**, whose conductivity and stability were significantly improved in comparison to that of **Zn-1**, which was used as a promising electrochemical biosensor for recognizing and distinguishing all the three common S-containing amino acids.

A thiophene derivative, 2,5-thiophene dicarboxylic acid (H_2L) was selected as a ligand to synthesize the Zn-MOFs, because thiophene and its derivatives are widely used as modified electrode materials for excellent electrochemical performance.[18–24] Upon reacting only H_2L with Zn^{2+} ions, colourless sheet crystals of **Zn-1** were obtained from the hydrothermal process (Fig. S1 and S2, ESI†). Single crystal X-ray diffraction reveals that **Zn-1** crystallizes in the monoclinic space group *P*2/*m*. The asymmetric unit consists of a penta-coordinated Zn^{2+} ion and a hexa-coordinated Zn^{2+} ion, two L^- ligands, one μ_2-O bridge and three H_2O molecules. Zn1 is penta-coordinated by O atoms from two L^- ligands, two water molecules and a μ_2-O atom. Zn2 is hexa-coordinated by O atoms from four L^- ligands, one water molecule and a μ_2-O atom. And a $\{Zn_2C_4O_8\}$ cluster is formed. This binuclear cluster is further extended along the *b* and *c* axes by the ligands L^- to afford a 2D plane (Fig. 1). However, during the electrochemical test, the cyclic voltammetry of **Zn-1** is unstable and unreproducible, and the powder X-ray diffraction (PXRD) measurements show that **Zn-1** is decomposed during the test.

When examining the structure of **Zn-1**, we proposed that the unstable **Zn-1** originated due to two reasons: (i) the insufficient coordination of the Zn^{2+} ion, which had the vacant coordination position and could be easily attacked by the solvent molecules and (ii) the parallelogram conformation of the framework in

[a] *Scientific Instrument Center, Shanxi University, Taiyuan, Shanxi 030006, China*
[b] *Department of Chemistry and Key Laboratory of Advanced Energy Materials Chemistry (MOE), College of Chemistry, Nankai University, Tianjin 300071, China. E-mail: qiuxh@nankai.edu.cn, mvbasten@nankai.edu.cn*

† Electronic supplementary information (ESI) available: Synthesis, structural characterizations, PXRD, electrochemical characterizations and other data for **Zn-1** and **Zn-2**. CCDC 1889630 and 1889631. For ESI and crystallographic data in CIF or other electronic formats see DOI: 10.1039/c9cc01701a

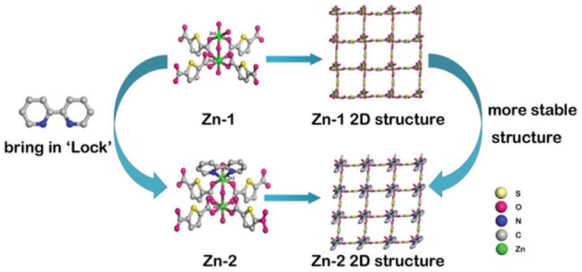

Fig. 1 Coordination environments, 2D structures and the conversion process of **Zn-1** and **Zn-2**.

Zn-1, which was variable and might be collapsed due to the solvent and/or electric current. Based on the above considerations, we introduced an auxiliary ligand, 2,2′-dipyridyl (bipy), as a 'lock', to improve the electrochemical stability of the Zn-L framework, as shown in Fig. 1. We chose several single crystals of **Zn-1** to react with the auxiliary ligand bipy in a glass bottle at 90 °C for 2 days, and a new 2D Zn-MOF (**Zn-2**) with the formula of $[Zn_2(L)_2(bipy)(\mu_2\text{-}O)(H_2O)_2]_n$ was obtained as block colorless crystals (Fig. S3, ESI†). **Zn-2** could also be obtained directly by a hydrothermal method from a mixture of $Zn(NO_3)_2{\cdot}6H_2O$, H_2L and bipy. The conversion of **Zn-1** to **Zn-2** was confirmed by the PXRD method (Fig. S4, ESI†).

Crystals of **Zn-2** obtained from either the conversion of **Zn-1** or from the direct synthesis were suitable for single crystal X-ray diffraction study, which reveals that **Zn-2** crystallizes in the triclinic space group $P\bar{1}$. The asymmetric unit consists of two hexa-coordinated Zn^{2+} ions, two L^- ligands, one μ_2-O bridge, one bipy molecule and two H_2O molecules. Zn1 is hexa-coordinated by four O atoms and two N atoms from two L^- ligands, one water molecule, a μ_2-O atom and one bipy molecule. Zn2 is hexa-coordinated by O atoms from four L^- ligands, one water molecule and a μ_2-O atom. And a $\{Zn_2C_4N_2O_8\}$ cluster is formed. This binuclear cluster is further extended along the *b* and *c* axes by the ligands L^- to afford a 2D plane (Fig. 1). **Zn-2** shows quite similar conformation to that of **Zn-1**, while bipy substitutes one of the coordination water molecules in **Zn-1**, and configures as a "lock" to clamp the Zn1 ion and replenish the coordination sites of Zn1 ions in **Zn-2**. On the other hand, the bipy ligands also act as a bridge that strut each parallelogram unit of the framework and restrains its deformation due to the steric hindrance. Benefiting from the introduction of the ligand lock, **Zn-2** exhibits extreme solvent stability in common organic solvents for at least two weeks, as proved by PXRD (Fig. S5, ESI†).

The electrochemical behavior of **Zn-2** was characterized by cyclic voltammetry (CV) measurements after coating unmodified **Zn-2** on the surface of a clean Au electrode (**AuE**, Φ = 1 mm). The CV curves of the MOF coated electrode, named as **Zn-2/AuE**, in DMF-$BMIMBF_4$ solution are shown in Fig. 2. As can be seen, a pair of quasi-reversible peaks were observed with E_{pa} = −1.23 V and E_{pc} = −1.06 V *versus* Ag/AgCl, which were attributed to the Zn^{2+}/Zn^{+} redox process.[25–27] The peak to peak separations (ΔE_p) were 0.17 V, and the half-wave potential was −1.15 V. The CVs on **Zn-2/AuE** were carried out for further thirty circles. The peak current density almost did not decrease, and this indicated good

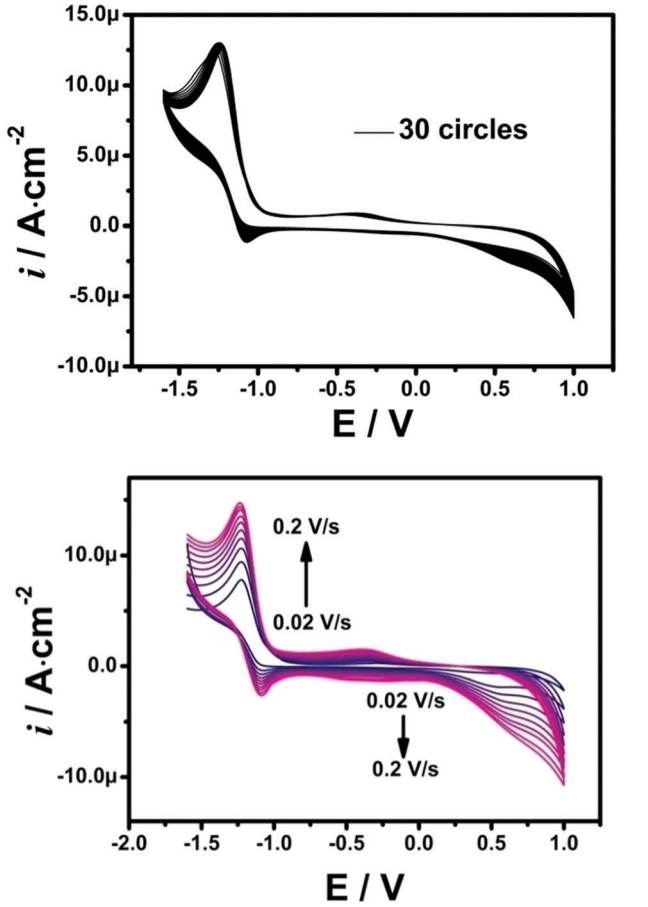

Fig. 2 (a) Cyclic voltammetry in DMF-BMIMBF4 solution of **Zn-2/AuE** for 30 circles and (b) cyclic voltammograms of **Zn-2/AuE** in DMF-BMIMBF4 at different scan rates from 0.02 V s^{-1} to 0.2 V s^{-1}.

reproducibility that originated from the high stability of **Zn-2**. The influence of scan rates (ν) was investigated too. The CVs of **Zn-2/AuE** in DMF-$BMIMBF_4$ solution with a scan rate from 0.02 V s^{-1} to 0.2 V s^{-1} are shown in Fig. 2b. The peak current densities of both the oxidation and reduction processes increase gradually with the increasing scan rates. The anodic (i_{pa}) and cathodic (i_{pc}) peak current densities are directly proportional to $\nu^{1/2}$ (see ESI†), which indicates a surface controlled process.[25]

Subsequently, **Zn-2/AuE** was used for discriminating three S-containing amino acids, L-cysteine (L-Cys), L-methionine (L-Met) and L-cystine (L-Cys–Cys). In an organism, S-containing amino acids used as mediate to attend most the effects of reactive oxygen species (ROS) on proteins. L-Cys is a non-essential amino acid and thus is one of the building blocks required for the synthesis of proteins.[26] L-Met and L-Cys–Cys in combination with other biomolecules have changed the serum or plasma cholesterol concentration to avoid the hepatoma-induced hyperlipidemia.[27] Thus, exploring convenient detection methods for S-containing amino acids is of great significance in food chemistry and medicine fields.[28–30] Many technologies have been exploited for detecting S-containing amino acids including fluorometry,[31,32] high performance liquid chromatography (HPLC) spectrophotometry,[33,34] capillary electrophoresis,[35,36] chemoluminescence methods,[37]

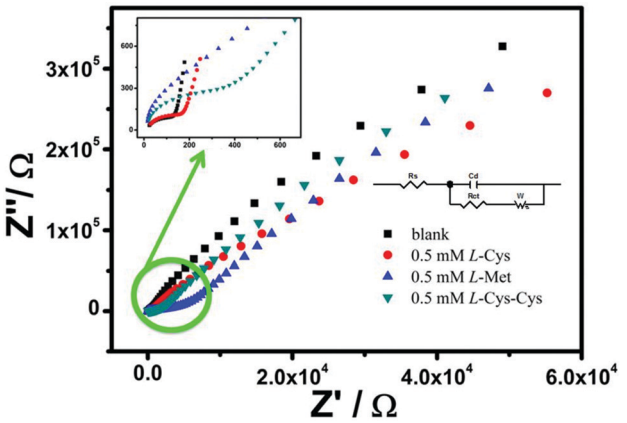

Fig. 3 Nyquist plots of **Zn-2/AuE** in DMF-BMIMBF4 solution or containing 0.5 mM L-Cys, L-Met and L-Cys–Cys, respectively. Inset: An equivalent circuit and a detailed graph.

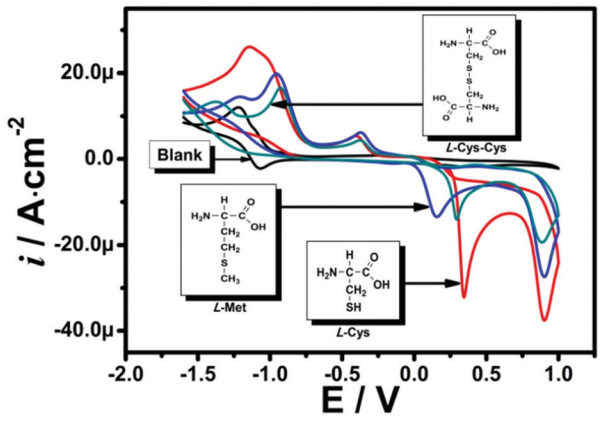

Fig. 4 Cyclic voltammograms of **Zn-2/AuE** in DMF-BMIMBF4 solution obtained in the presence of 0.5 mM of L-Cys, L-Met and L-Cys–Cys, respectively.

and nuclear magnetic resonance spectroscopy (NMR),[38] and these require expensive instruments and/or complex operation steps. In our work, **Zn-2** was used as electrode materials for recognizing and distinguishing three S-containing amino acids without any post-modification. To the best of our knowledge, this is the first observation of an electrochemical biosensor based on MOF materials for the recognition and distinction of all the three S-containing amino acids.[39–42]

The interaction between the three S-containing amino acids and **Zn-2** was further investigated by electrochemical impedance spectroscopy (EIS) and CV measurement. First, to characterize the proton conductivity of the **Zn-2/AuE** electrode, EIS analysis was performed on **Zn-2/AuE** in blank DMF-BMIMBF4 solution or containing L-Cys, L-Met and L-Cys–Cys, respectively (Fig. 3). The diameter of the semicircle represents the charge transfer resistance (R_{et}), the values of which correspond to blank, 0.5 mM L-Cys, 0.5 mM L-Cys–Cys, 0.5 mM L-Met and were 0.01, 2.78, 15.55 and 18.98 Ω cm^2, respectively. This shows that the electron conducting ability at the **Zn-2/AuE** interface descends following the sequence L-Cys, L-Cys–Cys and L-Met, which could be due to different chemically specific interactions between the frameworks and the different positions of the S atom in the corresponding S-containing amino acid guest molecules, which is further confirmed by the CV measurements (Fig. 4).

Fig. 4 shows the CV responses of **Zn-2/AuE** in DMF-BMIMBF$_4$ solution/suspension with 0.5 mM L-Cys, L-Met and L-Cys–Cys, respectively. The same reduction peak I at E_{pc} = 0.901 V is exhibited by all the three complexes, while the corresponding current density increases following the sequence of L-Cys ($i_{p,I1}$ = 2.5 × 10^{-5} A cm^{-2}) > L-Met ($i_{p,I2}$ = 1.8 × 10^{-5} A cm^{-2}) > L-Cys–Cys ($i_{p,I3}$ = 1.3 × 10^{-5} A cm^{-2}). In contrast, another reduction peak II for the three S-containing amino acids appeared at different potential positions (L-Cys at 0.35 V, L-Cys–Cys at 0.29 V and L-Met at 0.16 V with the highest current density of 1.25 × 10^{-5} A cm^{-2}) which can thus be used for distinguishing them easily. The EIS data and the CV responses confirm that the electron conducting abilities of the three S-containing amino acids at the **Zn-2/AuE** electrode are different from each other, which should be attributed to the different positions of the S atom in these three amino acids.

The impedance data of the three kinds of amino acids, L-Cys, L-Cys–Cys and L-Met, are 2.78, 15.55 and 18.98 Ω cm^2, respectively, which indicate that the mass transfer difficulty of these three substances on **Zn-2** follows the order of L-Cys > L-Cys–Cys > L-Met. As per the CV graphs, the potentials of reduction peak II are 0.35, 0.29 and 0.16 V for L-Cys, L-Cys–Cys and L-Met, respectively, which suggests that in a CV loop, the reduction degree of the three kinds of amino acids on **Zn-2** is in the order of L-Cys > L-Cys–Cys > L-Met, which corresponds well with the performance of the impedance test. This sequential change could be attributed to the different locations and configurations of the S atoms in these three kinds of amino acids. L-Cys has a terminal –SH group, which interacts easily with **Zn-2**; and L-Cys–Cys has an S–S bond, which tends to fracture. During the electrochemical process, some of L-Cys–Cys can decompose into L-Cys, as confirmed by further experiments (see the figures and explanations given in the ESI†), which also makes L-Cys–Cys interact with **Zn-2** easily. In contrast, when the –S–CH$_3$ group is present in L-Met, the steric hindrance of –CH$_3$ is much greater than that of –H, and thus the reduction reaction between L-Met and **Zn-2** is limited, although –CH$_3$ is an electron-donating group and is helpful for increasing the reactivity of S atoms.

Upon increasing the concentration of L-Cys, L-Met and L-Cys–Cys in the range from 0.2 mM to 0.6 mM, the current densities of peak II increase gradually for the three S-containing amino acids. The i_{pc} exhibits a nearly linear variation as the concentration of L-Cys, L-Met and L-Cys–Cys following the equations:

$$i_{pc} = -3.992 \times 10^{-5}\, c_{\text{L-Cys}} - 4.085 \times 10^{-6},\ R^2 = 0.997$$

$$i_{pc} = -3.258 \times 10^{-5}\, c_{\text{L-Met}} - 1.188 \times 10^{-6},\ R^2 = 0.992$$

$$i_{pc} = -2.302 \times 10^{-5}\, c_{\text{L-Cys-Cys}} - 6.900 \times 10^{-6},\ R^2 = 0.996$$

where i_{pc} is the cathodic peak current of peak II; $c_{\text{L-Cys}}$, $c_{\text{L-Met}}$ and $c_{\text{L-Cys-Cys}}$ are the concentrations of L-Cys, L-Met and L-Cys–Cys (A cm^{-2}); and R is the correlation coefficient. The sensitivity of L-Cys, L-Met and L-Cys–Cys are 39.92 μA M^{-1}, 32.58 μA M^{-1}

and 23.02 μA M^{-1}, and the detection limits of them are 3.12 μM, 1.93 μM and 2.05 μM, respectively, which are calculated according to the method mentioned in previous reports.[43] This result confirms that **Zn-2/AuE** can distinguish the three S-containing amino acids from both potential and current.

In summary, we have successfully synthesized new 2D Zn-MOFs. Through a method to introduce a ligand lock *via* a crystal-to-crystal process, the stability of the 2D framework was significantly improved, which was used as an electrochemical biosensor for recognizing and distinguishing three S-containing amino acids with excellent electrochemical performance. This is the first attempt to directly apply MOFs as electrochemical biosensors to recognize S-containing amino acids. We provide a promising method for the design of MOF sensors and the modification of electrochemical properties in electrochemistry and biochemistry.

This project was financially supported by the NFSC (21671111 and 21771112) and the NFS of Tianjin (17JCYBJC17700). We are also very grateful for the test platform provided by Shanxi University of Scientific Instrument Center.

Conflicts of interest

There are no conflicts to declare.

Notes and references

1 X. H. Liu, J. G. Ma, Z. Niu, G. M. Yang and P. Cheng, *Angew. Chem., Int. Ed.*, 2015, **54**, 988.
2 J. R. Li, R. J. Kuppler and H. C. Zhou, *Chem. Soc. Rev.*, 2009, **38**, 1477.
3 Z. Hu, B. J. Deibert and J. Li, *Chem. Soc. Rev.*, 2014, **43**, 5815.
4 H. Furukawa, K. E. Cordova, M. O'Keeffe and O. M. Yaghi, *Science*, 2013, **341**, 1230444.
5 M. Eddaoudi, D. F. Sava, J. F. Eubank, K. Adil and V. Guillerm, *Chem. Soc. Rev.*, 2015, **44**, 228.
6 A. H. Chughtai, N. Ahmad, H. A. Younus, A. Laypkov and F. Verpoort, *Chem. Soc. Rev.*, 2015, **44**, 6804.
7 F.-Y. Yi, D. Chen, M.-K. Wu, L. Han and H.-L. Jiang, *ChemPlusChem*, 2016, **81**, 675.
8 L. K. Yang, T. X. Huang, Z. C. Zeng, M. H. Li, X. Wang, F. Z. Yang and B. Ren, *Nanoscale*, 2015, **7**, 18225.
9 Z. Xu, L. Yang and C. Xu, *Anal. Chem.*, 2015, **87**, 3438.
10 R. R. Salunkhe, Y. V. Kaneti and Y. Yamauchi, *ACS Nano*, 2017, **11**, 5293.
11 P. Ling, J. Lei, L. Zhang and H. Ju, *Anal. Chem.*, 2015, **87**, 3957.
12 P. Ling, J. Lei, L. Jia and H. Ju, *Chem. Commun.*, 2016, **52**, 1226.
13 L. Liu, Y. Zhou, S. Liu and M. Xu, *ChemElectroChem*, 2018, **5**, 6.
14 D. M. D'Alessandro, *Chem. Commun.*, 2016, **52**, 8957.
15 W. J. Ma, Q. Jiang, P. Yu, L. F. Yang and L. Q. Mao, *Anal. Chem.*, 2013, **85**, 7550.
16 M. S. Yao, W. X. Tang, G. E. Wang, B. Nath and G. Xu, *Adv. Mater.*, 2016, **28**, 5229.
17 M. S. Yao, X. J. Lv, Z. H. Fu, W. H. Li, W. H. Deng, G. D. Wu and G. Xu, *Angew. Chem., Int. Ed.*, 2017, **56**, 16510 (*Angew. Chem.*, 2017, **129**, 16737).
18 P. C. Mahakul, K. Sa, B. V. R. S. Subramanyam, K. C. Patra and P. Mahanandia, *J. Mater. Sci.*, 2018, **53**, 8151.
19 M. Daneshpour, B. Karimi and K. Omidfar, *Biosens. Bioelectron.*, 2018, **109**, 197.
20 H. Zejli, K. Y. Goud and J. L. Marty, *Talanta*, 2018, **185**, 519.
21 Y. H. Kwon, J. J. Park, L. M. Housel, K. Minnici, G. Y. Zhang, S. R. Lee, S. W. Lee, Z. M. Chen, S. Noda, E. S. Takeuchi, K. J. Takeuchi, A. C. Marschilok and E. Reichmanis, *ACS Nano*, 2018, **12**, 3126.
22 B. Singh, R. A. Doong, D. S. Chauhan, A. K. Dubey and Anshumali, *Mater. Chem. Phys.*, 2017, **205**, 462.
23 T. Darmanin and F. Guittard, *Prog. Polym. Sci.*, 2014, **39**, 656.
24 X. Q. Wu, J. G. Ma, H. Li, D. M. Chen, W. Gu, G. M. Yang and P. Cheng, *Chem. Commun.*, 2015, **51**, 9161.
25 Y. Xu, X. B. Yin, X. W. He and Y. K. Zhang, *Biosens. Bioelectron.*, 2015, **68**, 197.
26 M. Li and M. Dincă, *J. Am. Chem. Soc.*, 2011, **133**, 12926.
27 M. Kawasaki, Y. Miura, R. Funabiki and K. Yagasaki, *Biosci., Biotechnol., Biochem.*, 2010, **74**, 158.
28 L. Yang, S. Kinoshita, T. Yamada, S. Kanda, H. Kitagawa, M. Tokunaga, T. Ishimoto, T. Ogura, R. Nagumo, A. Miyamoto and M. Koyama, *Angew. Chem., Int. Ed.*, 2010, **49**, 5348.
29 N. Clemente Plaza, M. Reig Garcia-Galbis and R. M. Martinez-Espinosa, *Molecules*, 2018, **23**, 575.
30 Z. Z. Yin, S. W. Cheng, L. B. Xu, H. Y. Liu, K. Huang, L. Li, Y. Y. Zhai, Y. B. Zeng, H. Q. Liu, Y. Shao, Z. L. Zhang and Y. X. Lu, *Biosens. Bioelectron.*, 2018, **100**, 565.
31 B. K. Rani and S. A. John, *Biosens. Bioelectron.*, 2016, **83**, 237.
32 C. Y. Zeng, X. L. Zhang and L. Pu, *Chem. – Eur. J.*, 2017, **23**, 2432.
33 G. Upert, G. Mourier, A. Pastor, M. Verdenaud, D. Alili, D. Servent and N. Gilles, *Chem. Commun.*, 2014, **50**, 8408.
34 S. Murillo-Sanchez, D. Beaufils, J. M. G. Manas, R. Pascal and K. Ruiz-Mirazo, *Chem. Sci.*, 2016, **7**, 3406.
35 X. Chen, J. A. Rao, J. Wang, J. J. Gooding, G. Zou and Q. J. Zhang, *Chem. Commun.*, 2011, **47**, 10317.
36 S. Jezierski, V. Tehsmer, S. Nagl and D. Belder, *Chem. Commun.*, 2013, **49**, 11644.
37 Y. C. Yu, J. J. Shi, X. C. Zhao, Z. Q. Yuan, C. Lu and J. Lu, *Analyst*, 2016, **141**, 3305.
38 E. Ferrari, R. Grandi, S. Lazzari, G. Marverti, M. C. Rossi and M. Saladini, *Polyhedron*, 2007, **26**, 4045.
39 G. Ziyatdinova, E. Kozlova and H. Budnikov, *Electrochim. Acta*, 2018, **270**, 369.
40 F. Chekin, S. Bagheri and S. B. Abd Hamid, *J. Chin. Chem. Soc.*, 2015, **62**, 689.
41 E. Sharifi, A. Salimi and E. Shams, *Bioelectrochemistry*, 2012, **89**, 9.
42 J. B. Raoof, R. Ojani, H. Beitollahi and R. Hosseinzadeh, *Anal. Sci.*, 2006, **22**, 1213.
43 J. Heinze, *Angew. Chem., Int. Ed. Engl.*, 1984, **23**, 831.

